

Antiferromagnetic Resonance Studies on the Spin-Canted Molecular Magnet β -*p*-NCC₆F₄CNSSN

Antonio Alberola,[†] Christopher M. Pask,[†] Jeremy M. Rawson,^{*,‡} Eric J. L. McInnes,[‡] Joanna Wolowska,[‡] Hassane El Mkami,[⊥] and Graham Smith[⊥]

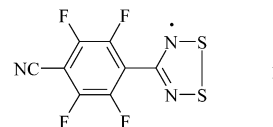
The Department of Chemistry, The University of Cambridge, Lensfield Road, Cambridge CB2 1EW, U.K., EPSRC cw-EPR service, The Department of Chemistry, The University of Manchester, Oxford Road, Manchester M13 9PL, U.K., and The School of Physics and Astronomy, University of St Andrews, Fife KY16 9AJ, U.K.

Received: October 9, 2003; In Final Form: October 21, 2003

Multifrequency (24–94 GHz) and variable temperature (5–300 K) single-crystal electron paramagnetic resonance (EPR) studies have been used to probe the magnetic exchange pathway, spin dynamics, and assignment of the principal magnetic axes in the organic molecular magnet 4-(4'-cyano-tetrafluorophenyl)-1,2,3,5-dithiadiazolyl, β -*p*-NCC₆F₄CNSSN. Orientation-dependent studies indicate that the dominant exchange pathway is perpendicular to the crystallographic *c*-axis, while variable-temperature studies confirm the ordering transition at 36 K and illustrate that the sublattice magnetization is essentially saturated below 15 K. The orientation dependence of the EPR spectra at 5 K has confirmed the easy axis of magnetization to be parallel to the *b*-axis and allowed the first determination of the intermediate and hard axes of magnetization as parallel to *c*- and *a*-axes, respectively.

Electron paramagnetic resonance (EPR) spectroscopy has proved an invaluable tool in the field of molecule-based magnetic materials.¹ It has often been used in conjunction with theoretical calculations to provide reliable estimates of the spin density distribution in organic radicals,² which may otherwise only be accessed via more arduous methods, for example, polarized neutron diffraction.³ In addition, it provides direct access to the electronic structure of single molecule magnets (spin ground state and zero-field splitting parameters necessary to elucidate the energy barrier to spin reorientation).⁴ In comparison, EPR has not been applied as extensively to the study of magnetically ordered molecular materials, although the theory of the EPR spectra of magnetically ordered systems is established.⁵ Single-crystal EPR studies of magnetically ordered systems can provide information on the ordering temperature, the type of the magnetic order (e.g., ferro- or antiferromagnetism), the magnetic anisotropy, and orientation of the magnetic axes. Additional information on the spin dynamics can also be extracted. Few EPR studies on magnetically ordered phases of molecular materials have been reported, and they have focused on the magnetic ground state of some fullerene⁶ derivatives including the ferromagnet C₆₀TDAE (*T*_c = 16 K) and a number of TTF (TTF = tetrathiafulvalene) derivatives,⁷ which order as antiferromagnets around 10 K. Here we describe single-crystal EPR studies on the β -polymorph of the organic magnet *p*-NCC₆F₄CNSSN (**1**).

Previous studies⁸ have shown that **1** (Figure 1) orders as a canted antiferromagnet below 36 K with a canting angle of ca. 0.1°. Symmetry constraints restrain the spontaneous moment to lie in the *ab* plane, but subsequent powder neutron diffraction



studies⁹ could not unambiguously determine whether the easy axis of magnetization was parallel to *a* or *b*; the best fit to the data was consistent with the easy axis of magnetization parallel to the crystallographic *b*-axis rather than the *a*-axis.

The current communication illustrates how EPR spectroscopy can provide detailed information on the magnetic exchange pathway and the spin dynamics of the magnetically ordered phase and allows an unambiguous assignment of not only the easy axis but also the intermediate and hard axes of magnetization.

Needle-like crystals of **1** up to 30 mm long in which the crystallographic *c*-axis corresponds to the needle axis of the crystal were prepared according to the literature method. Preliminary single-crystal EPR studies on **1** were recorded at Q-band (ca. 34 GHz) and W-band (ca. 94 GHz) with the needle axis of the crystal perpendicular to the applied field, that is, with the applied field at a fixed but arbitrary angle in the *ab* plane. The temperature dependence of the W-band EPR spectra is shown in Figure 2. At both Q- and W-band frequencies, no marked changes in the spectra were observed on cooling to 40 K despite a broad maximum in χ in the SQUID data,⁸ consistent with a short-range ordering phenomenon. An abrupt decrease in the resonance field was observed at 36 K due to the onset of magnetic order, which gives rise to an internal magnetic field. The normal resonance condition ($h\nu = g\mu_B\mathbf{H}_{\text{appl}}$) no longer holds and two new resonances, both associated with the ordered phase, are anticipated.⁵ These two resonances are functions of both the applied field, \mathbf{H}_{appl} , and the internal field, \mathbf{H}_{int} (as well as crystal orientation). At W-band, only the lower field resonance is observed, the high-field resonance could not be detected even

* To whom correspondence should be addressed. E-mail: jmr31@cus.cam.ac.uk.

[†] The University of Cambridge.

[‡] The University of Manchester.

[⊥] University of St. Andrews.

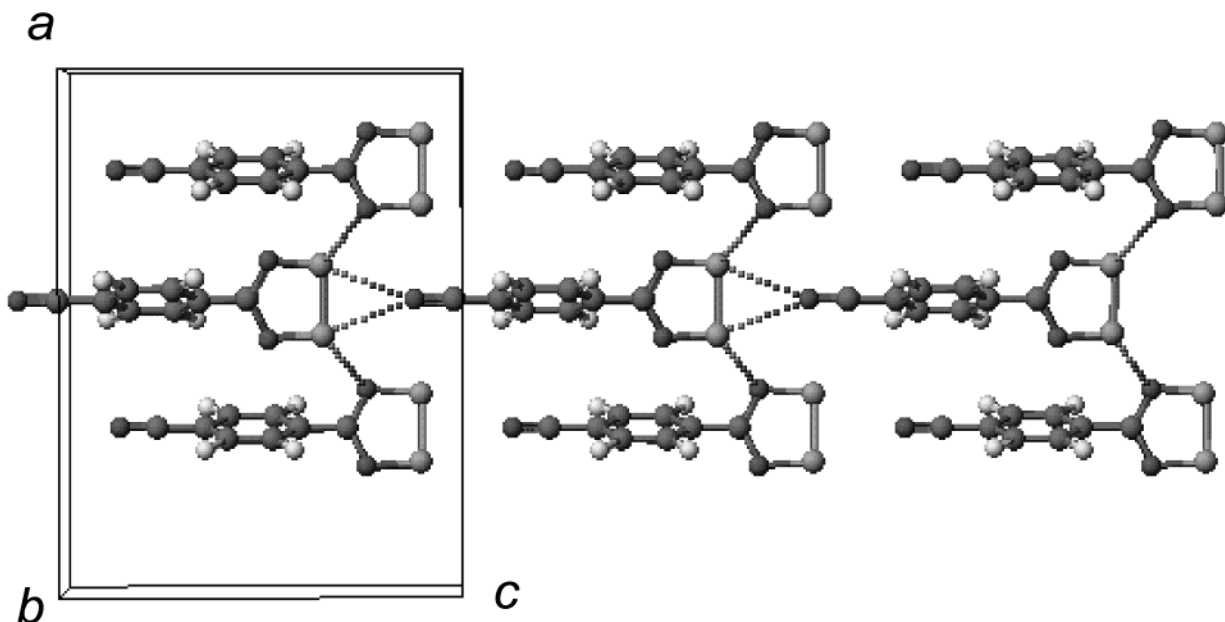


Figure 1. Structure of 1β .

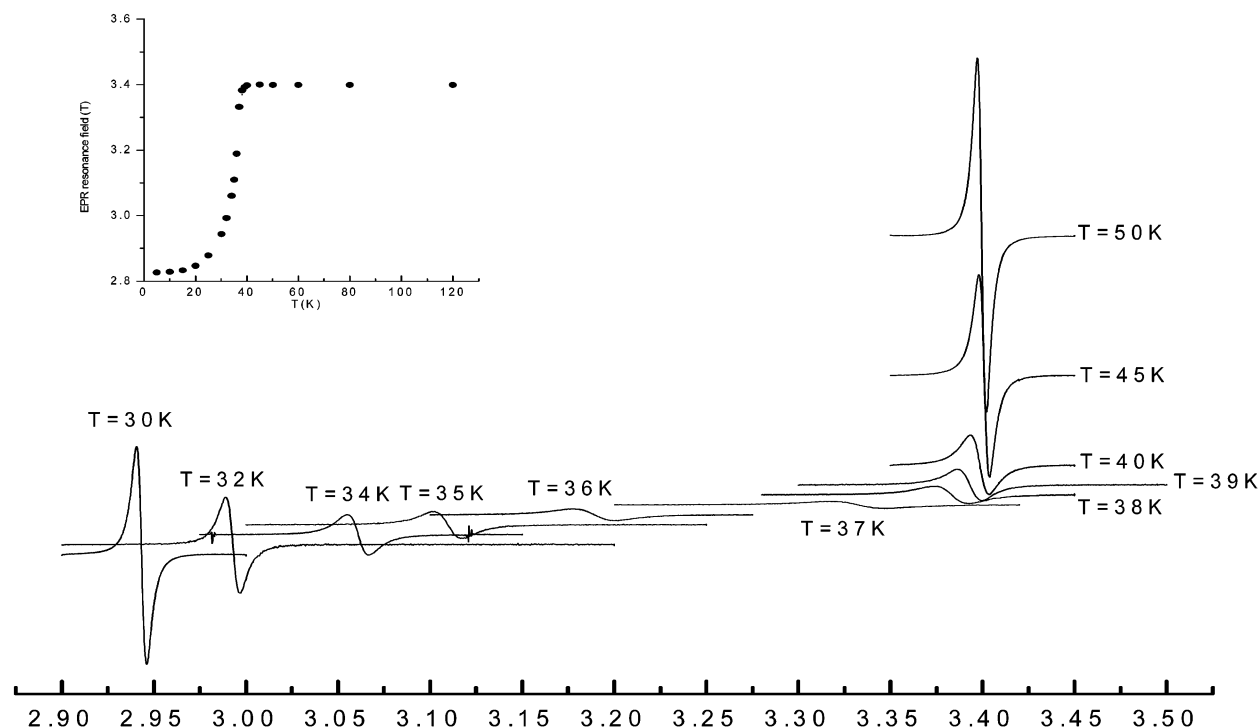


Figure 2. Temperature dependence of the W-band EPR spectra of 1β at a fixed angle with respect to the magnetic field (in tesla) in the ab plane. The inset shows the temperature dependence of the resonance position.

down to 5 K but is estimated to occur at very high fields (in excess of 10 T).

Similar behavior was found at Q-band, but now this high field resonance could also be observed below 20 K but still occurred above the operating field of the EPR electromagnet at $T > 20$ K. Both resonances moved to low field on cooling. Since the resonance frequency below T_N becomes a function of \mathbf{H}_{int} as well as \mathbf{H}_{appl} , it exhibits a strong temperature dependence because the internal field follows closely the order parameter, α ($\alpha = 1$ at $T = 0$ K decreasing to 0 when $T = T_N$). A plot of the temperature dependence of the shift in the resonance field (in reduced units) at both Q- and W-band frequencies shows an excellent fit to the Brillouin function

(Figure 3). Below 15 K, the ordering of the magnetic sublattices is essentially complete.

The temperature dependence of the line width (Figure 4) at both frequencies also exhibits an abrupt variation at T_N with substantial line-broadening on cooling to 36 K but sharpening rapidly on cooling below 36 K. Dipolar coupling is a common source of line broadening in EPR spectroscopy, whereas exchange coupling tends to have the opposite effect and lead to line narrowing.¹⁰ The narrowing of the line width below T_N is due to the dominant effect of the exchange coupling (which is usually orders of magnitude greater than dipolar coupling) below T_N . Additional measurements at W-band with the applied field parallel to the needle axis show a less marked temperature

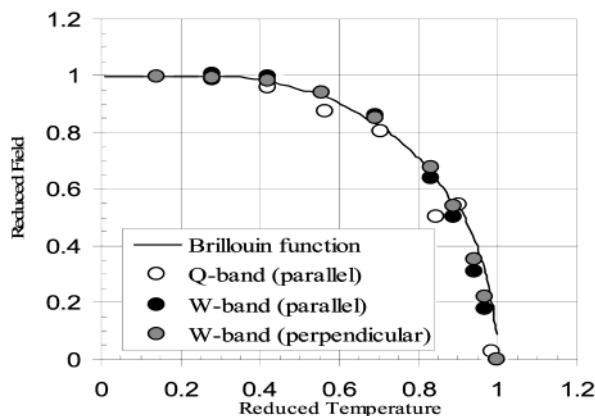


Figure 3. Shift in the resonance field within and perpendicular to the crystallographic *ab* plane as a function of temperature in reduced units. The solid line represents the Brillouin function for $S = 1/2$.

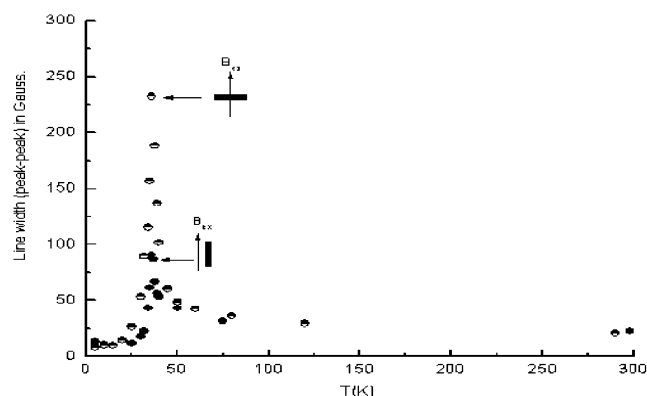


Figure 4. Temperature dependence of the line width (W-band) with the applied field parallel and perpendicular to the needle axis (crystallographic *c*-axis).

dependence of the line width. These observations are entirely consistent with previous models of the magnetic exchange pathway,¹¹ which indicate that magnetic exchange along the crystallographic *c*-axis via CN \cdots S contacts (see Figure 1) is negligible. Dipolar coupling exhibits an r^{-3} distance dependence, so the long intermolecular separation of radical centers along the *c*-axis (11.933 Å) leads to comparatively narrow line widths.

In contrast the greater line width perpendicular to the *c*-axis is consistent with stronger dipolar coupling arising from close intermolecular S \cdots N contacts (3.488 Å) between radicals in different chains. Similar effects have been previously observed.¹²

Under orthorhombic symmetry, the magnetic axes must be coincident with the crystallographic axes. Orientation-dependent studies at K-band (24 GHz) and Q-band around the crystallographic *c*-axis at 5 K show sinusoidal modulation of the resonant field for both the high-frequency and low-frequency resonances (Figure 5) with maxima and minima separated by $\pi/2$, indicating that these extrema coincide with the principal magnetic axes. The orientation dependence of pure antiferromagnets is strongly dependent on the axis of rotation.⁷ The in-phase oscillations of both high- and low-field resonances in the

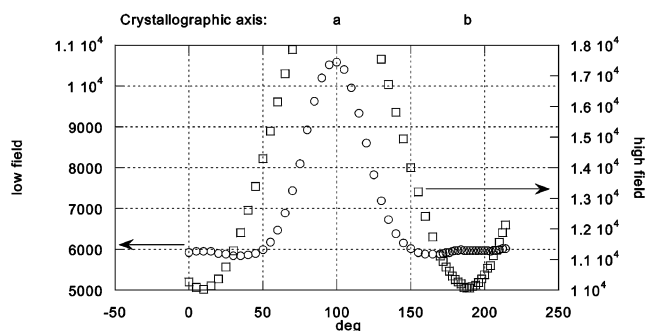


Figure 5. Rotation pattern of 1β around the crystallographic *c*-axis at Q-band at 5 K.

current case are typical for rotation of an antiferromagnet about its intermediate axis.

Thus the crystallographic *c*-axis corresponds to the intermediate axis of magnetization with the magnetic easy axis (resonance minimum) parallel to the *b*-axis.

A determination of the anisotropy field and spin-flop field from a full frequency/field/orientation analysis will be the subject of a future report.

Acknowledgment. One of us (J.M.R.) thanks Prof. P. Turek for enthusiastic discussions, which prompted us to undertake this study. We thank the EPSRC (C.M.P. and A.A.) and Gates Cambridge Trust (A.A.) for financial support.

References and Notes

- (1) Bencini, A.; Gatteschi, D. *EPR of Exchange Coupled Systems*; Springer: Berlin, 1990.
- (2) (a) Chen, P.; DeBeer George, S.; Cabrito, I.; Antholine, W. E.; Moura, J. J. G.; Moura, I.; Hedman, B.; Hodgson, K. O.; Solomon, E. I. *J. Am. Chem. Soc.* **2002**, *124*, 744. (b) Cirujeda, J.; Vidal-Gancedo, J.; Jürgens, O.; Mota, F.; Novoa, J. J.; Rovira, C.; Veciana, J. *J. Am. Chem. Soc.* **2000**, *122*, 11393.
- (3) (a) Carling, S. G.; Visser, D.; Hautot, D.; Watts, I. D.; Day, P.; Ensling, J.; Gutlich, P.; Long, G. J.; Grandjean, F. *Phys. Rev. B* **2002**, *66*, 104407. (b) Pontillon, Y.; Bencini, A.; Caneschi, A.; Dei, A.; Gatteschi, D.; Gillon, D.; Sangregorio, C.; Stride, J.; Totti, F. *Angew. Chem., Int. Ed.* **2000**, *39*, 1786.
- (4) (a) Sessoli, R.; Gatteschi, D. *Angew. Chem., Int. Ed.* **2003**, *42*, 268. (b) Aubin, S. M. J.; Sun, Z.; Pardi, L.; Krzystek, J.; Folting, K.; Brunel, L. C.; Rheingold, A. L.; Christou, G.; Hendrickson, D. N. *Inorg. Chem.* **1999**, *38*, 5329.
- (5) (a) Nagamiya, T. *Prog. Theor. Phys.* **1954**, *11*, 309. (b) Kittel, C. *Introduction to Solid State Physics*, 7th. ed.; Wiley: New York, 1996.
- (6) Arcon, D.; Prassides, K. *π -electron magnetism, Structure and bonding*; Springer-Verlag: Berlin, 2001; Vol. 100.
- (7) (a) Coulon, C.; Scott, J. C.; Laversanne, R. *Phys. Rev. B* **1986**, *33*, 6235. (b) Coulon, C.; Laversanne, R.; Amiel, J.; Delhaes, P. *J. Phys. C: Solid State Phys.* **1986**, LT753.
- (8) Banister, A. J.; Bricklebank, N.; Lavender, I.; Rawson, J. M.; Gregory, C. I.; Tanner, B. K.; Clegg, W.; Elsegood, M. R. J.; Palacio, F. *Angew. Chem., Int. Ed. Engl.* **1996**, *35*, 2533.
- (9) Palacio, F.; Antorrena, G.; Castro, M.; Burriel, R.; Rawson, J. M.; Smith, J. N. B.; Bricklebank, N.; Novoa, J.; Ritter, C. *Phys. Rev. Lett.* **1997**, *79*, 2336.
- (10) Carlin, R. L. *Magnetochemistry*; Springer-Verlag: Berlin, 1986.
- (11) Langley, P. J.; Rawson, J. M.; Smith, J. N. B.; Schuler, M.; Schweiger, A.; Palacio, F.; Antorrena, G.; Hoffman, C.; Quintel, A.; Rechsteiner, P.; Hülliger, J. *J. Mater. Chem.* **1999**, *9*, 1431.
- (12) Caneschi, A.; Gatteschi, D.; Renard, J. P.; Rey, P.; Sessoli, R. *Inorg. Chem.* **1989**, *28*, 1976.